



Title	Diffusion mechanism of sodium ions in compacted montmorillonite under different NaCl concentration
Author(s)	Kozaki, Tamotsu; Liu, Jinhong; Sato, Seichi
Citation	Physics and Chemistry of the Earth, Parts A/B/C, 33(14-16), 957-961 <a href="https://doi.org/10.1016/j.pce.2008.05.007">https://doi.org/10.1016/j.pce.2008.05.007</a>
Issue Date	2008
Doc URL	<a href="http://hdl.handle.net/2115/47464">http://hdl.handle.net/2115/47464</a>
Type	article (author version)
File Information	PCE33-14-16_957-961.pdf



[Instructions for use](#)

**For Physics and chemistry of the earth**

(to be presented at Migration'07)

## **Diffusion Mechanism of Sodium Ions in Compacted Montmorillonite under Different NaCl Concentration**

Tamotsu KOZAKI\*<sup>1)</sup>, Jinhong LIU<sup>1,2)</sup>, and Seichi SATO<sup>1)</sup>

1) Division of Energy and Environmental Systems, Graduate School of Engineering, Hokkaido University,  
N13 W8, Kita-ku, Sapporo, 060-8628, Japan

2) Chinergy Company Ltd., B-916, Chuangxin Bldg., Tsinghua Science Park, Haidian District, Beijing,  
100084, China (current address)

\*Corresponding author,

TEL: +81 11 706 6687

FAX: +81 11 706 6688

E-mail: kozaki@eng.hokudai.ac.jp (T. Kozaki)

## Abstract

Compacted bentonite, the major mineral being montmorillonite, is a candidate buffer material for geological disposal of high-level radioactive waste. The diffusion behavior of radionuclides in the compacted montmorillonite is an important issue to be clarified for the safety assessment of geological disposal. In this study, one-dimensional, non-steady diffusion experiments using  $^{22}\text{Na}$  at different diffusion temperatures and the measurement of the basal spacings by XRD were conducted for Na-montmorillonite saturated with NaCl solutions of different concentrations. Some basal spacings of the montmorillonite were found to decrease from 1.88 to 1.56 nm as the NaCl concentration increased from 0 to 0.1 M. The apparent self-diffusion coefficients at 298 K obtained in this study slightly increased as the NaCl concentration increased from 0 to 0.5 M, while the activation energies, calculated from the temperature dependences of the diffusion coefficients, were found to be 14, 22, and 17 kJ mol<sup>-1</sup> at NaCl concentrations of 0, 0.1, and 0.5 M, respectively. These NaCl concentration dependences of the diffusion coefficients and their activation energies can be explained by assuming three independent diffusion processes (diffusion in pore water, on external surface of montmorillonite, and in interlayer of montmorillonite).

Keywords: Bentonite, montmorillonite, self-diffusion, sodium-22, geological disposal, radioactive waste

## 1. Introduction

Compacted bentonite is the most promising buffer material for geological disposal of high-level radioactive waste (Pusch and Yong, 2006). An important function of the compacted bentonite is to retard the transport of radionuclides from waste forms to the surrounding host rock after degradation of overpack. Due to the very low hydraulic conductivity of the bentonite, the radionuclide transport in the disposal system is considered to be mainly governed by diffusion. Therefore, it is essential to clarify the diffusion behavior of radionuclides in compacted bentonite under repository conditions - conditions in which relatively higher temperatures and groundwater with high ionic strength could be expected (JNC, 2000). However, the diffusion of radionuclides in compacted bentonite is regarded to be very complicated since it could be influenced by many parameters, such as the microstructures of the bentonite, the degree of compaction, the accessory minerals in the bentonite, pore water chemistry, and the types of exchangeable cations present.

Sodium, being a typical monovalent cation, is a suitable ion for modeling transport. It also plays an important role in the diffusion of radionuclides as an exchangeable cation of Na-bentonite. Many experimental results are available for Na<sup>+</sup> diffusion in compacted bentonite (Glaus *et al.*, 2007; Kozaki *et al.*, 1998, 2005; Liu *et al.*, 2003; Molera and Eriksen, 2002; Muurinen *et al.*, 1990; Van Loon *et al.*, 2005a, b). In addition, several diffusion models (Bourg *et al.*, 2006, 2007; Lehikoinen *et al.*, 1998; Ochs *et al.*, 2001) have been studied and computer simulations (Chang *et al.*, 1995; Prayongphan *et al.*, 2006) have been performed to explain the diffusion behavior of cations.

The activation energy for diffusion, which can be calculated from the temperature dependence of the

diffusion coefficients, is an important parameter elucidating the diffusion process. However, to the best knowledge of present authors, there are no reports available on the study of the ionic strength dependence of the activation energy for  $\text{Na}^+$  diffusion in compacted bentonite. In this study, therefore, the apparent self-diffusion coefficients of  $^{22}\text{Na}^+$  ions were determined under different temperatures and NaCl concentrations. This report examines the NaCl concentration dependence of activation energy for  $^{22}\text{Na}^+$  diffusion together with the microstructure of the water-saturated, compacted bentonite observed by the X-ray diffraction (XRD) method.

## **2. Experimental**

The bentonite used in this study was homoionized Na-montmorillonite that was prepared from Kunipia-F (a product of Kunimine Industries Co. Ltd.) by three successive immersion of the bentonite in a fresh solution of 1 M NaCl. Excess NaCl salt was removed by rinsing the bentonite with distilled water through a dialysis tube (Viskase Sales, UC36-32-100) until no  $\text{Cl}^-$  ions were detected with an  $\text{AgNO}_3$  solution. The bentonite was dried in an oven at 378 K, mortared with a pestle, and then sieved to obtain a powder with aggregate sizes between 75 and 150  $\mu\text{m}$ . The montmorillonite content and the cation exchange capacity (CEC) of the Na-montmorillonite as received were more than 98 % (Ito *et al.*, 1993) and 1.13 eq / kg-clay (Kozai *et al.*, 1993), respectively.

The powdered Na-montmorillonite was compacted into 20 mm-diameter acrylic resin cells to obtain a dry density of 1.0  $\text{kg dm}^{-3}$ . The cells were then saturated with NaCl solutions having NaCl concentrations from 0.01 to 0.5 M. The cell lengths were 20 mm for the diffusion experiments and 10 mm for the XRD

measurements. The water content of the montmorillonite was 0.4 (gram of H<sub>2</sub>O / gram of dry montmorillonite).

The basal spacing of the compacted bentonite in the solution-saturated state was determined from XRD profiles measured from 3 to 8 degrees of 2 $\theta$  using an X-ray diffraction apparatus (Rigaku RU-300) equipped with a copper cathode. Flat diffraction planes were obtained by sectioning the samples soon after they were removed from a water saturation cell.

The apparent self-diffusion coefficients of <sup>22</sup>Na<sup>+</sup> in the montmorillonite were determined by one-dimensional, non-steady diffusion experiments (so-called *back-to-back* diffusion method). In these diffusion experiments, a small amount of <sup>22</sup>NaCl radiotracer was applied to one end of a montmorillonite sample cell. Diffusion of the tracer was allowed to proceed by placing two montmorillonite specimens in contact as illustrated in Fig. 1. Five runs having temperatures of 288 to 323 K were made, but the temperature of each run was held constant. After a prescribed period of time for diffusion, each cell was disassembled and the montmorillonite specimens were sectioned into 0.5-mm-thick slices as the specimen was extruded progressively from the cell. The relative radioactivity of <sup>22</sup>Na was measured for each slice with a well-type NaI scintillation counter.

The apparent self-diffusion coefficients of <sup>22</sup>Na<sup>+</sup> ions were obtained from the concentration profile measurements of the radiotracer in the montmorillonite samples. The activation energies (*E<sub>a</sub>*) were determined from the temperature dependences of the apparent diffusion coefficients.

The detailed procedures of montmorillonite homoionization, compaction, water-saturation of the

montmorillonite sample, XRD measurement, and the diffusion experiment are described elsewhere (Kozaki *et al.*, 1998).

### 3. Results and discussion

#### 3.1. Basal spacings of montmorillonite

Figure 2 shows XRD profiles of the compacted Na-montmorillonite saturated with NaCl solutions of different concentrations. At the  $1.0 \text{ kg dm}^{-3}$  dry density studied here, 1.88 nm basal spacings were observed in all specimens exposed for all NaCl concentrations, while weak 1.56 nm basal spacing peaks were found in the specimens having NaCl concentrations of 0.1 and 0.5 M. In a previous study for compacted Na-montmorillonite saturated with distilled water at different dry densities (Kozaki *et al.*, 1998), basal spacings of 1.88 nm at dry densities from 1.0 to  $1.5 \text{ kg dm}^{-3}$  and of 1.56 nm at dry densities from 1.4 to  $1.8 \text{ kg dm}^{-3}$  were observed, whereas neither of the diffraction peaks were obtained at dry densities below  $1.0 \text{ kg dm}^{-3}$ . The basal spacings of 1.88 and 1.56 nm correspond to a three-water-layer state and a two-water-layer hydrate state, respectively, of the interlayer (interlamellar) spaces of montmorillonite (Watanabe and Sato, 1988). It should be noted here that quasicrystals (well-arranged montmorillonite tactoids), which can be detected by the XRD method, emerged at a dry density of  $1.0 \text{ kg dm}^{-3}$ . In addition, the results of this study suggest that a relatively high NaCl concentration solution, 0.1 M and above, can remove water molecules from the interlayers of the montmorillonite tactoids. This results in the shrinkage of the interlayers and the increases in the number of the quasicrystals (the number of interlayers).

#### 3.2. Diffusion coefficient and its activation energy

A typical concentration profile of  $^{22}\text{Na}^+$  is shown in Figure 3. The apparent self-diffusion coefficients of  $^{22}\text{Na}^+$  in compacted Na-montmorillonite saturated with NaCl solutions are summarized in Table 1. Figure 4 shows self-diffusion coefficients of  $^{22}\text{Na}^+$  as a function of NaCl concentrations. The diffusion coefficients of  $^{22}\text{Na}^+$  were found to increase slightly as the NaCl concentrations increased from 0 to 0.5 M. Muurinen *et al.* (1990) reported an apparent diffusion coefficient of  $\text{Na}^+$  of  $5.0 \times 10^{-11} \text{ m}^2 \text{ s}^{-1}$  at a dry density of  $1.8 \text{ kg dm}^{-3}$  and an apparent diffusion coefficient of  $3.0 \times 10^{-10} \text{ m}^2 \text{ s}^{-1}$  at a dry density of  $0.8 \text{ kg dm}^{-3}$  for MX-80 bentonite. Molera and Eriksen (2002) reported almost constant values of apparent diffusion coefficients around  $5 \times 10^{-11} \text{ m}^2 \text{ s}^{-1}$  for MX-80 bentonite at a dry density of  $1.8 \text{ kg dm}^{-3}$  and under NaCl concentrations from 0.05 M to 1 M. Although some experimental conditions were different, these values are consistent with those obtained in the present study.

The activation energies for the diffusion obtained from the temperature dependences of  $^{22}\text{Na}$  self-diffusion at each NaCl concentration are listed in Table 1. The dependence of activation energies on NaCl concentration is shown in Fig. 5. This shows there are different values of the activation energy; about  $14 \text{ kJ mol}^{-1}$  at a NaCl concentration of 0 M, about  $22 \text{ kJ mol}^{-1}$  at NaCl concentrations of 0.1 and 0.2 M, and about  $17 \text{ kJ mol}^{-1}$  at NaCl concentrations of 0.4 and 0.5 M. Considering higher and lower activation energies than that for  $\text{Na}^+$  diffusion in free water ( $18.4 \text{ kJ mol}^{-1}$  (Parsons, 1959)), at least two diffusion processes other than free water diffusion in clay pore should be taken into account to interpret the changes in activation energy as a function of NaCl concentration.

### 3.3 Diffusion processes in montmorillonite

Three possible diffusion pathways for cations in compacted, water-saturated, montmorillonite can be envisaged; the pore water, the external surfaces of montmorillonite aggregates, and the interlayer (interlamellar) spaces (Pusch *et al.*, 2001). If these diffusion pathways have independent diffusion roles in montmorillonite samples, the total diffusion flux of Na<sup>+</sup> ions in water-saturated, compacted montmorillonite (mol m<sup>-2</sup> s<sup>-1</sup>),  $J_{tot}$ , can be expressed by the following equation:

$$J_{tot} = J_p + J_s + J_i \quad (1)$$

where  $J_p$ ,  $J_s$ , and  $J_i$  are the diffusion flux in pore water, on the external surface, and in the interlayer of montmorillonite (mol m<sup>-2</sup> s<sup>-1</sup>), respectively.

For the self-diffusion of <sup>22</sup>Na<sup>+</sup> ions in Na-montmorillonite where the specific radioactivity gradient of <sup>22</sup>Na is the driving force for diffusion, the total apparent self-diffusion coefficient of <sup>22</sup>Na<sup>+</sup> ions in the water-saturated, compacted montmorillonite (m<sup>2</sup> s<sup>-1</sup>),  $D_{tot}$ , can be expressed as follows;

$$D_{tot} = x_p g_p D_p + x_s g_s D_s + x_i g_i D_i \quad (2)$$

where  $x_p$ ,  $x_s$ , and  $x_i$  are the mole fractions of Na<sup>+</sup> ions in the different diffusion pathways;  $g_p$ ,  $g_s$ , and  $g_i$  are the geometrical factors of the corresponding pathways;  $D_p$ ,  $D_s$ , and  $D_i$  are the apparent diffusion coefficients of Na<sup>+</sup> in each pathways; and the subscripts  $p$ ,  $s$ , and  $i$ , represent the pore water, the external surface, and the interlayer spacing, respectively.

For the diffusion coefficient of pore water,  $D_p$ ,  $1.35 \times 10^{-9}$  m<sup>2</sup> s<sup>-1</sup> was reported as the diffusivity of Na<sup>+</sup> ions in free water, together with an activation energy for their diffusion of 18.4 kJ mol<sup>-1</sup> (Parsons, 1959). Similarly,  $D_s$  was reported to be  $3.7 \times 10^{-10}$  m<sup>2</sup> s<sup>-1</sup> from experimental results conducted for a

clay-suspension, together with an activation energy of  $13 \text{ kJ mol}^{-1}$  (Dufey and Laudelout, 1975). The value of  $D_i$  at 300 K was estimated to be  $1.8 \times 10^{-10} \text{ m}^2 \text{ s}^{-1}$  for the three-water-hydrate state and  $5.1 \times 10^{-10} \text{ m}^2 \text{ s}^{-1}$  for the two-water-hydrate state using a molecular dynamics simulation (Chang *et al.*, 1995). An activation energy around  $23 \text{ kJ mol}^{-1}$  was reported for the diffusion in highly compacted montmorillonite ( $1.8 \text{ kg dm}^{-3}$ ), where major pathways were considered to be the interlayers with a two-water-layer hydrate state (Kozaki *et al.*, 1998). As the different diffusion coefficients and their activation energies are reported for each diffusion pathway, the predominant term on the right side of equation (2) may shift from one term to another as parameters are influenced by changes in NaCl concentration. If this occurs, the activation energy for diffusion can also change as a function of NaCl concentration.

The geometrical factors ( $g_p$ ,  $g_s$ , and  $g_i$ ), which are considered to be altered by changes in NaCl concentration, cannot be evaluated separately in diffusion experiments. However, we can assume the relation  $g_p \approx g_i$  since these two diffusion pathways can be considered to be parallel (Bourg, 2004, Bourg *et al.*, 2007). With the same reason, the relation  $g_i \approx g_s$  can be assumed, resulting in the similar values among the three factors,  $g_p \approx g_s \approx g_i$ . On the other hand, the mole fractions of  $\text{Na}^+$  ions in each diffusion pathway ( $x_p$ ,  $x_s$ , and  $x_i$ ) are very sensitive to changes in NaCl concentration. For example, if the same number of  $\text{Na}^+$  ions as in the cation exchange capacity (CEC) of montmorillonite is assumed to be present on the external surfaces and in the interlayer spaces, the fraction of  $\text{Na}^+$  ions in the pore water,  $x_p$ , increases with NaCl concentration according to the following equation:

$$x_p = 1 - \frac{CEC}{CEC + I \cdot m_w / \rho_w} \quad (3)$$

where  $m_w$  is the ratio of weight of water to 1 kg of montmorillonite ( $=W / (1-W)$ ) (-);  $W$  is the water content (-);  $I$  is the NaCl concentration in solution ( $\text{mol m}^{-3}$ ); and  $\rho_w$  is the density of water ( $\text{kg m}^{-3}$ ). The calculated values of  $x_p$  are listed in Table 2. The values of  $x_p$  increase from less than 1% to 23% as NaCl concentrations increase from 0.001 to 0.5 M. On the other hand, the remaining  $\text{Na}^+$  ions, *i.e.*,  $(1 - x_p)$ , cannot be divided quantitatively into the two remaining fractions,  $x_s$  and  $x_i$ , due to insufficient information on the microstructure of the water-saturated, compacted montmorillonite. Note that the XRD peak of the three-water-hydrate states (1.88 nm) emerged at the dry density of  $1.0 \text{ kg dm}^{-3}$ , but no peak below this dry density (Kozaki *et al.*, 2001). This suggests that the montmorillonite at this dry density has the lowest amount of stacking montmorillonite layers (*i.e.* quasicrystal) to produce the diffraction peak. In addition, when NaCl concentration increases at this dry density, a portion of stacking layers could lose water molecules from their interlayers, resulting in the decrease of the basal spacing, as described above. Simultaneously, randomly oriented layers can coagulate and to form stacks (Suzuki *et al.*, 2005). Therefore, it can be supposed that as the NaCl concentration increases at this dry density,  $x_s$  decreases and  $x_i$  increases.

According to equation (2) and the parameters discussed above, the predominant diffusion process at very low NaCl concentration (about 0) can be estimated to be the diffusion on the external surfaces (the second term on the right side in equation (2)), which has an activation energy of  $13 \text{ kJ mol}^{-1}$  (Dufey and Laudelout, 1975). This can be attributed mainly to the high value of  $x_s$ . Note that at this low NaCl concentration, a thick electrical double layer can develop on the montmorillonite surface. The thickness of

the layer can be more than 10 nm, which is comparable with the maximum average pore spacings (15.9 nm) at a dry density of  $1.0 \text{ kg dm}^{-3}$  (Kozaki *et al.*, 2001). This thick electrical double layer could provide good connectivity of the diffusion pathways for surface diffusion. At intermediate NaCl concentration, around 0.1 M, the predominant diffusion process can be considered as changing from external surface diffusion to interlayer diffusion (the third term on the right side in equation (2)). This change is reasonable since the surface diffusion cannot increase at this higher NaCl concentration due to the lower value of  $x_s$  and the collapse of the electrical double layer caused by the relatively higher NaCl concentration. On the other hand, when the NaCl concentration reaches 0.3 M and above, the value of  $x_p$  becomes greater than  $x_i$  and  $x_s$ , and the product of  $x_p$ ,  $g_p$ , and  $D_p$  can overcome the other terms. This means that the predominant diffusion process changes from interlayer diffusion to pore water diffusion (the first term on the right side of equation (2)), which has an activation energy of  $18.4 \text{ kJ mol}^{-1}$  (Parsons, 1959). In conclusion, the NaCl concentration dependence of the activation energy for  $^{22}\text{Na}^+$  diffusion, as shown in Fig. 5, can be explained by using equation (2) with appropriate parameters. Similarly, the NaCl concentration dependence of the self-diffusion coefficients of  $^{22}\text{Na}^+$ , as shown in Fig. 4, can also be approximately described by assuming a geometrical factor ( $g$ ) of  $1/3$ , along with equation (2) and appropriate parameters. The value of  $g$  used here corresponds to the parameter  $G = 3$ , which is recommended as an inversed geometric factor elsewhere (Kato *et al.*, 1995).

#### 4. Conclusions

For compacted Na-montmorillonite samples saturated with different concentrations of NaCl solutions,

one-dimensional, non-steady diffusion experiments using  $^{22}\text{Na}$  at different diffusion temperatures and the measurement of the basal spacings by XRD were conducted. The XRD measurements indicated that a small portion of the basal spacings of the montmorillonite decreased from 1.88 nm to 1.56 nm as the NaCl concentration increased from 0 to 0.1 M. On the other hand, the apparent self-diffusion coefficient at 298 K obtained in this study increased slightly as the NaCl concentration increased from 0 to 0.5 M. The activation energies, calculated from the temperature dependences of the diffusion coefficients, were found to be 14, 22, and 17 kJ mol<sup>-1</sup> at NaCl concentrations of 0, 0.1, and 0.5 M, respectively. These NaCl concentration dependences of the diffusion coefficients and their activation energies are consistent when assuming three independent diffusion processes (pore water diffusion, external surface diffusion, and interlayer diffusion) with appropriate parameters.

### **Acknowledgements**

This work has been partly performed in the Central Institute of Isotope Science, Hokkaido University. Financial support was provided by the Japan Atomic Energy Agency (JAEA), and the Radioactive Waste Management Funding and Research Center (RWMC).

### **References**

Bourg, I. C., 2004. Diffusion of water and inorganic ions in saturated compacted bentonite. PhD thesis, University of California, Berkeley.

- Bourg, I.C., Sposito, G., Bourg, A.C.M., 2007. Modeling cation diffusion in compacted water-saturated sodium bentonite at low ionic strength. *Environmental Science and Technology* 41 (23), 8118-8122.
- Bourg, I.C., Sposito, G., Bourg, A.C.M., 2006. Tracer diffusion in compacted, water-saturated bentonite. *Clays and Clay Minerals* 54 (3), 363-374.
- Chang, F.-R.C., Skipper, N.T., Sposito, G., 1995. Computer simulation of interlayer molecular structure in sodium montmorillonite hydrates. *Langmuir* 11 (7), 2734-2741.
- Dufey, J.E., Laudelout, H.G., 1975. Self-diffusion of sodium on clay surface as influenced by two other alkali cations. *Journal of Colloid and Interface Science* 52 (2), 340-344.
- Glaus, M.A., Baeyens, B., Bradbury, M.H., Jakob, A., Van Loon, L.R., Yaroshchuk, A., 2007. Diffusion of  $^{22}\text{Na}$  and  $^{85}\text{Sr}$  in montmorillonite: Evidence of interlayer diffusion being the dominant pathway at high compaction. *Environmental Science & Technology* 41 (2), 478-485.
- Ito, M., Okamoto, M., Shibata, M., Sasaki, Y., Danhara, T., Suzuki, K., Watanabe, T., 1993. Mineral composition analysis of bentonite. Tech. Rep., Power Reactor and Nuclear Fuel Development Corporation, PNC TN8430 93-003. (in Japanese)
- Japan Nuclear Cycle Development Institute (JNC), 2000. JNC Tech. Rep. H12: project to establish the scientific and technical basis for HLW disposal in Japan, supporting report 3 safety assessment of the geological disposal system, JNC TN1410 2000-04.

- Kato, H., Muroi, M., Yamada, N., Ishida, H., Sato, H., 1995. Estimation of effective diffusivity in compacted bentonite. *Mater. Res. Soc. Proc.* 353, 277-284.
- Kozai, N., Ohnuki, T., Muraoka, S., 1993. Sorption characteristics of neptunium by sodium-smectite. *Journal of Nuclear Science and Technology* 30 (11), 1153-1159.
- Kozaki, T., Fujishima, A., Saito, N., Sato, S., Ohashi, H., 2005. Effects of dry density and exchangeable cations on the diffusion process of sodium ions in compacted montmorillonite. *Engineering Geology* 81 (3), 246-254.
- Kozaki, T., Fujishima, A., Sato, S., Ohashi, H., 1998. Self-diffusion of sodium ions in compacted sodium montmorillonite. *Nuclear Technology* 121 (1), 63-69.
- Kozaki, T., Inada, K., Sato, S., Ohashi, H., 2001. Diffusion mechanism of chloride ions in sodium montmorillonite. *Journal of Contaminant Hydrology* 47 (2-4), 159-170.
- Lehikoinen, J., Muurinen, A., Olin, M., 1998. Ionic transport in compacted bentonite: preliminary equilibrium results. *Mater. Res. Soc. Proc.* 506, 383-390.
- Liu, J.H., Yamada, H., Kozaki, T., Sato, S., Ohashi, H., 2003. Effect of silica sand on activation energy for diffusion of sodium ions in montmorillonite and silica sand mixture. *Journal of Contaminant Hydrology* 61 (1-4), 85-93.
- Molera, M., Eriksen, T., 2002. Diffusion of  $^{22}\text{Na}^+$ ,  $^{85}\text{Sr}^{2+}$ ,  $^{134}\text{Cs}^+$  and  $^{57}\text{Co}^{2+}$  in bentonite clay compacted to different densities: experiments and modeling. *Radiochimica Acta* 90 (9-11), 753-760.

- Muurinen, A., Olin, M., Uusheimo, K., 1990. Diffusion of sodium and copper in compacted sodium bentonite at room temperature. *Mater. Res. Soc. Proc.* 176, 641-647.
- Ochs, M., Lothenbach, B., Wanner, H., Sato, H., Yui, M., 2001. An integrated sorption-diffusion model for the calculation of consistent distribution and diffusion coefficients in compacted bentonite. *Journal of Contaminant Hydrology* 47 (2-4), 283-296.
- Parsons, R., 1959. *Handbook of Electrochemical Constants*. Butterworths Sci. Publ., pp. 79
- Prayongphan, S., Ichikawa, Y., Kawamura, K., Suzuki, S., Chae, B.G., 2006. Diffusion with micro-sorption in bentonite: evaluation by molecular dynamics and homogenization analysis. *Computational Mechanics* 37 (4), 369-380.
- Pusch, R., Yong, R.N., 2006. *Microstructure of smectite clays and engineering performance*. Taylor & Francis, London & New York.
- Pusch, R., Moreno, L., Neretnieks, I., 2001. Microstructural modeling of transport in smectite clay buffer. *Proc. International Symposium on Suction, Swelling, Permeability and Structure of Clays- IS- Shizuoka 2001*, 47-51.
- Suzuki, S., Prayongphan, S., Ichikawa, Y., Chae, B.G., 2005. In situ observation of the swelling of bentonite aggregates in NaCl solution. *Applied Clay Science* 29, 89-98.
- Van Loon, L.R., Baeyens, B., Bradbury, M.H., 2005a. Diffusion and retention of sodium and strontium in Opalinus clay: Comparison of sorption data from diffusion and batch

sorption measurements, and geochemical calculations. *Applied Geochemistry* 20 (12), 2351-2363.

Van Loon, L.R., Muller, W., Iijima, K., 2005b. Activation energies of the self-diffusion of HTO,  $^{22}\text{Na}^+$  and  $^{36}\text{Cl}^-$  in a highly compacted argillaceous rock (Opalinus Clay). *Applied Geochemistry* 20 (5), 961-972.

Watanabe, T., Sato, T., 1988. Expansion characteristics of montmorillonite and saponite under various relative humidity conditions. *Clay Science* 7, 129-138.

Table and figure captions

Table 1 Apparent self-diffusion coefficients of  $^{22}\text{Na}^+$  and their activation energies obtained for the compacted Na-montmorillonite saturated with NaCl solutions of different NaCl concentrations

Table 2 Calculated values of the mole fraction of  $\text{Na}^+$  ions in the pore water at different NaCl concentrations

Figure 1 Schematic of diffusion cell

Figure 2 XRD profiles of the compacted Na-montmorillonite with a dry density of  $1.0 \text{ kg dm}^{-3}$  saturated with NaCl solutions of different concentrations. Dotted lines correspond to a basal spacing of 1.88 nm (left line) and of 1.56 nm (right line)

Figure 3 Concentration profile of  $^{22}\text{Na}^+$  in compacted Na-montmorillonite (Dry density:  $1.0 \text{ kg dm}^{-3}$ , NaCl concentration: 0.2 M, Diffusion temperature: 298 K, Diffusion period: 23.6 h,  $D_a: 1.2 \times 10^{-10} \text{ m}^2 \text{ s}^{-1}$ )

Figure 4 Self-diffusion coefficients of  $^{22}\text{Na}^+$  in compacted Na-montmorillonite as a function of NaCl concentrations

Figure 5 Activation energies for self-diffusion of  $^{22}\text{Na}^+$  in compacted Na-montmorillonite as a function of NaCl concentrations

Table 1

NaCl concentration [M]	Apparent self-diffusion coefficient [ $\text{m}^2 \text{s}^{-1}$ ]						$E_a$ [kJ mol $^{-1}$ ]
	278 K	288 K	298 K	303 K	313 K	323 K	
0(*)	$4.9 \times 10^{-11}$	$6.4 \times 10^{-11}$	$7.4 \times 10^{-11}$	$7.2 \times 10^{-11}$		$1.2 \times 10^{-10}$	$14.1 \pm 1.2$
	$4.2 \times 10^{-11}$	$6.4 \times 10^{-11}$		$7.7 \times 10^{-11}$		$1.1 \times 10^{-10}$	
0.05		$5.7 \times 10^{-11}$	$7.1 \times 10^{-11}$		$9.5 \times 10^{-11}$	$1.3 \times 10^{-10}$	$17.8 \pm 1.0$
		$5.8 \times 10^{-11}$	$8.3 \times 10^{-11}$		$1.0 \times 10^{-10}$	$1.4 \times 10^{-10}$	
0.1		$5.9 \times 10^{-11}$	$7.2 \times 10^{-11}$		$1.1 \times 10^{-10}$	$1.8 \times 10^{-10}$	$23.2 \pm 1.5$
		$6.2 \times 10^{-11}$	$7.7 \times 10^{-11}$		$1.2 \times 10^{-10}$	$1.6 \times 10^{-10}$	
0.2		$5.4 \times 10^{-11}$	$1.2 \times 10^{-10}$		$1.5 \times 10^{-10}$	$1.8 \times 10^{-10}$	$22.1 \pm 3.0$
		$7.6 \times 10^{-11}$	$9.5 \times 10^{-11}$		$1.4 \times 10^{-10}$	$1.8 \times 10^{-10}$	
0.4		$6.6 \times 10^{-11}$	$1.2 \times 10^{-10}$		$1.6 \times 10^{-10}$	$1.5 \times 10^{-10}$	$16.7 \pm 3.4$
		$9.2 \times 10^{-11}$	$9.5 \times 10^{-11}$		$1.2 \times 10^{-10}$	$2.0 \times 10^{-10}$	
0.5		$9.6 \times 10^{-11}$	$1.2 \times 10^{-10}$		$1.6 \times 10^{-10}$	$2.4 \times 10^{-10}$	$16.9 \pm 1.6$
		$1.0 \times 10^{-10}$	$1.2 \times 10^{-10}$		$1.6 \times 10^{-10}$	$1.9 \times 10^{-10}$	

(\*) Kozaki *et al.* (1998)

Table 2

NaCl concentration [M]	$x_p$ [-]
0	0
0.001	$6 \times 10^{-4}$
0.05	0.03
0.1	0.06
0.2	0.11
0.3	0.15
0.4	0.19
0.5	0.23

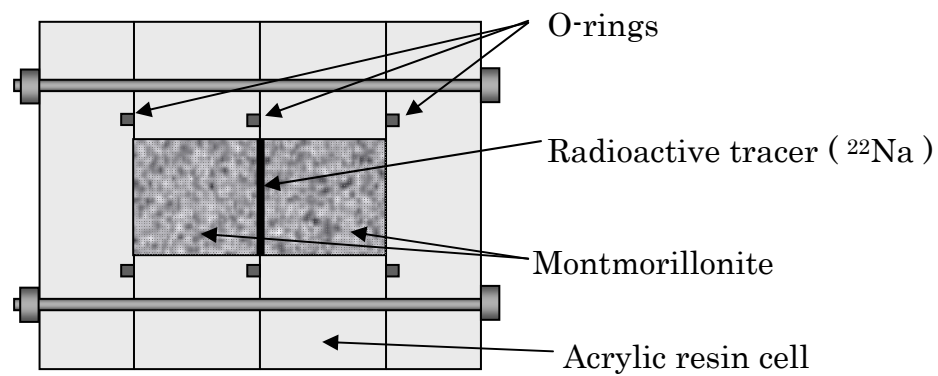


Figure 1

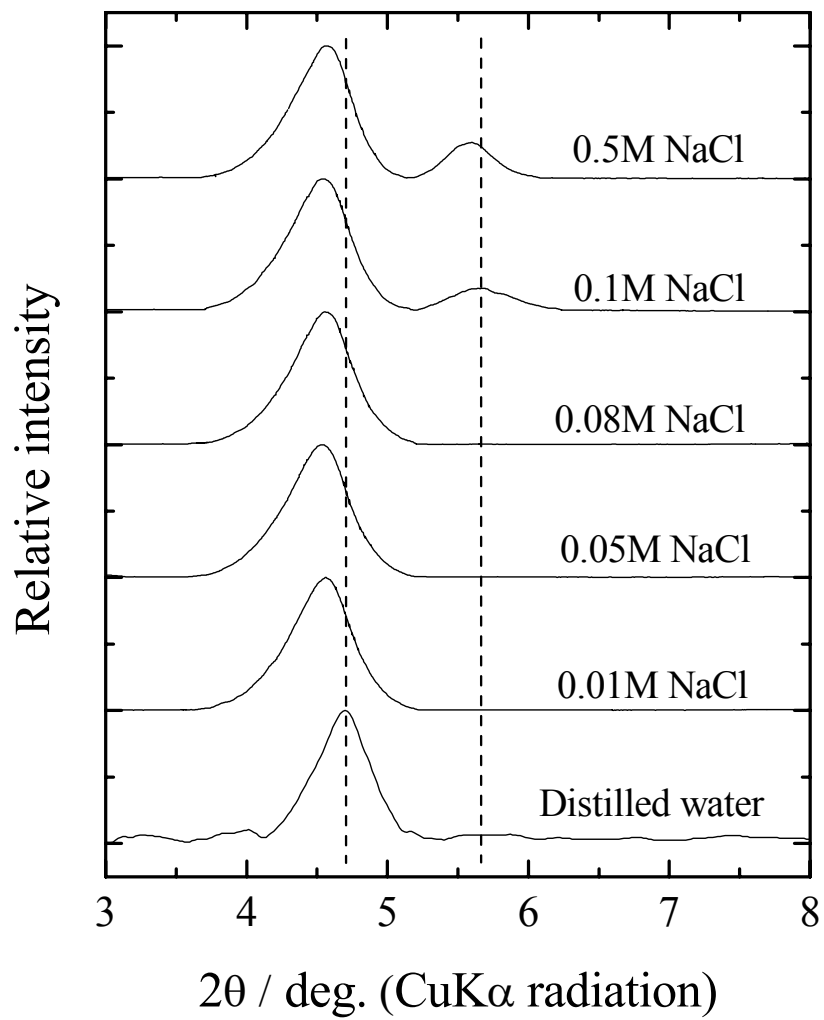


Figure 2

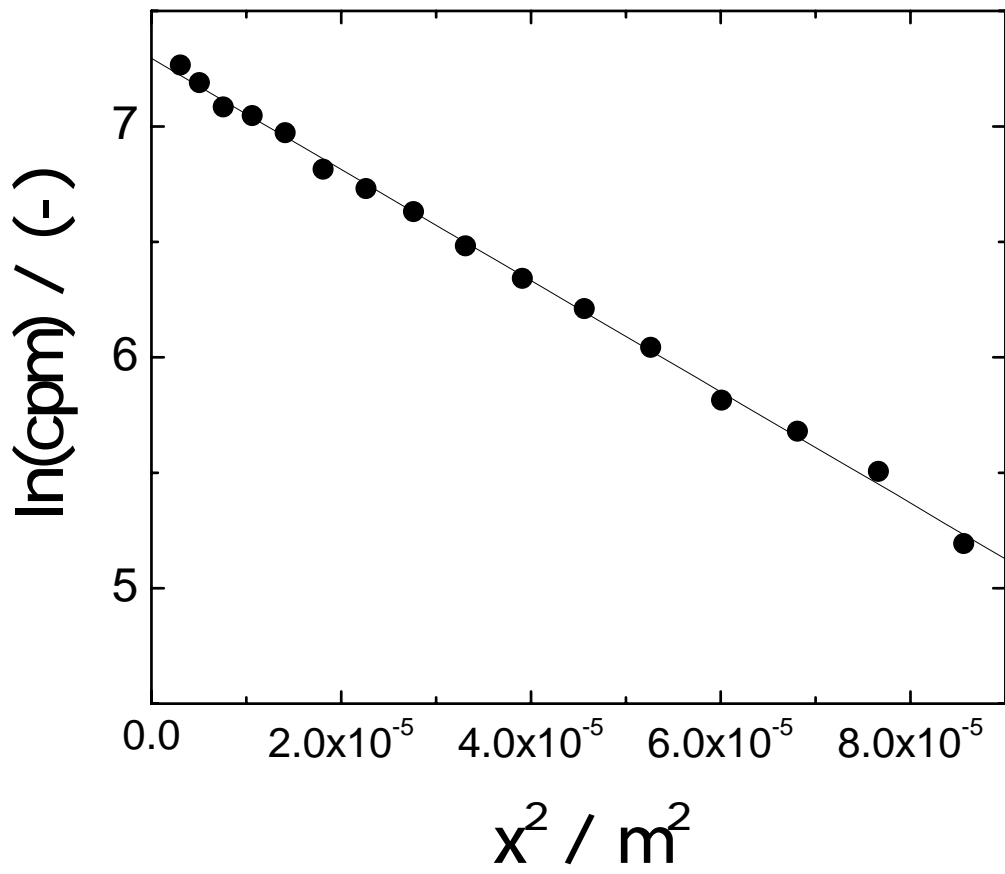


Figure 3

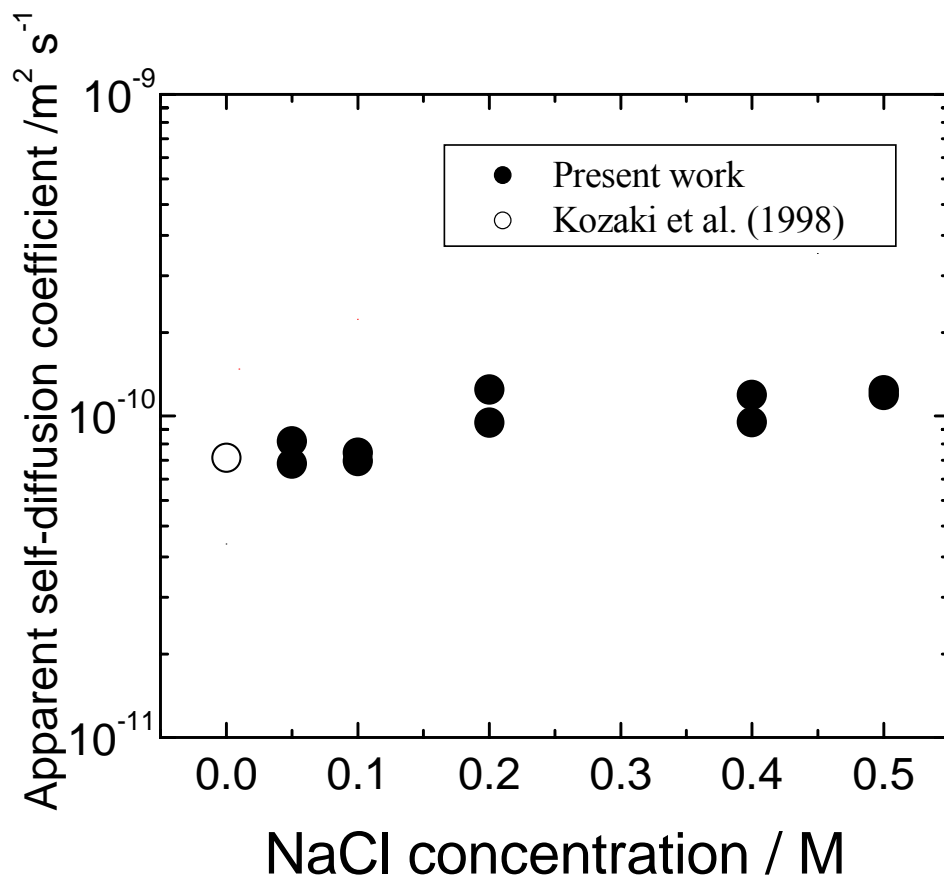


Figure 4

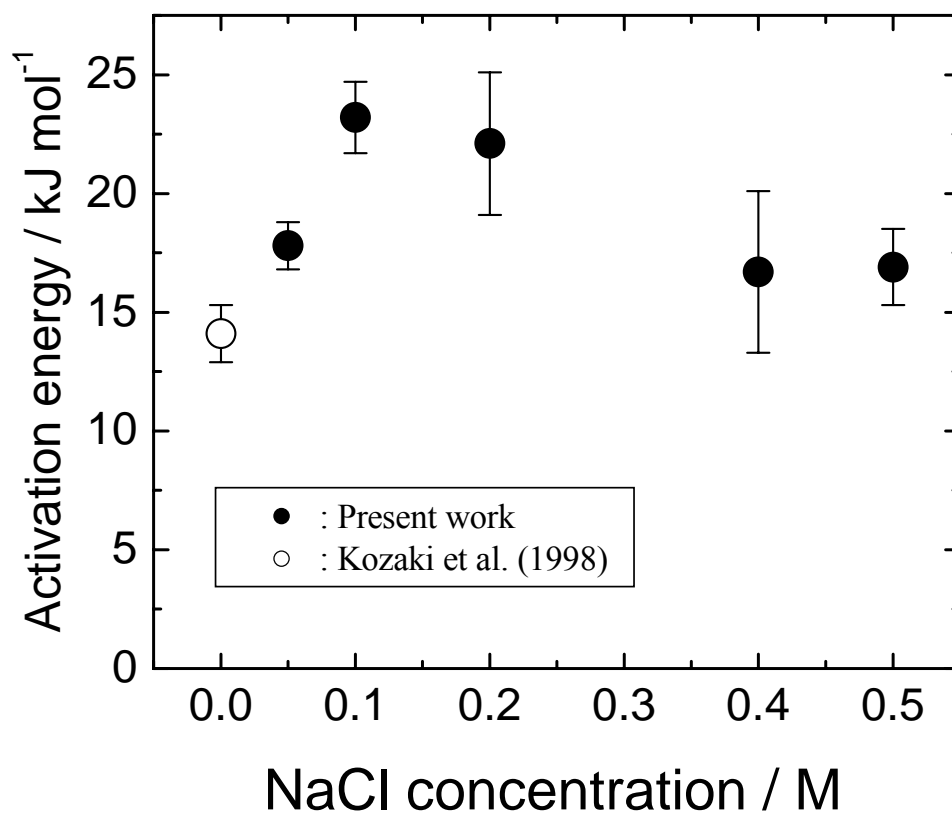


Figure 5